Supernumerary ice-crystal halos?

Michael V. Berry

Geometric-optics singularities in the intensity profiles of refraction halos formed by randomly oriented ice crystals are softened by diffraction and decorated with fine supernumerary fringes. If the crystals have a fixed symmetry axis (as in parhelia), the geometric singularity is a square-root divergence, as in the rainbow. However, the universal curve that describes diffraction is different from the rainbow's Airy function, with weak maxima (supernumerary fringes) on the geometrically dark region inside the halo (and even fainter fringes outside); these are much smaller than their counterparts on the light side of rainbows. If the crystals have no preferred orientation (as in the 22° halo), the geometric singularity is a step. In this case the universal diffraction function has no maxima, and its supernumeraries are shoulders rather than maxima. The low contrast of the fringes is probably the main reason why supernumerary halos are rarely if ever seen.

1. Introduction

It is well known[1,2] that both rainbows and ice-crystal halos are consequences of the minimum deviation of sunlight. The origins of the minima are, however, different in the two cases. In the rainbow, the rays through an individual raindrop have a minimum deviation at a directional caustic (corresponding to the Descartes ray), whereas in halos the rays through each crystal form a collimated beam, and the minimum is over beams from differently oriented crystals (this is the same phenomenon as the minimum deviation of a beam by a rotated prism, e.g., on a spectrometer turntable). In spite of this difference, at the level of geometric optics rainbows and halos share the property that their differential scattering cross sections, as functions of the deviation angle, possess singularities. For rainbows, this is an inverse square root (arising from the Jacobian of the mapping between angles of incidence and deviation, that is, from x to x^2). For halos, the form of the singularity (see Section 2) can be an inverse square root or a step, depending on the nature of the distribution of crystal orientations.

Geometric optics fails on fine scales, and in the case of the rainbow the intensity singularity is softened by diffraction according to $\mathrm{Ai}^2\{-\rho\}$, where Ai is the Airy function[3] and ρ is a scaled rainbow-crossing coordinate. The oscillations of $\mathrm{Ai}^2\{-\rho\}$ are the interference fringes that are visible as supernumerary rainbows on the bright side of the geometric maximum ($\rho > 0$). It is natural to ask what are the analogous diffraction modifications of the geometric singularities for halos and in particular whether there are supernumerary halos. These are the questions addressed here.

Minnaert[4] claimed that supernumerary halos "have been seen at times" but gave no details. Visser[5,6] employed diffraction theory to calculate their directions and claimed that diffraction is responsible for the observed wide variations in halo colors. I know of no recent evaluation of these claims, but the calculations that follow make it seem unlikely that halo fringes have been seen in nature. Können[7] suggests that observations previously interpreted as supernumerary halos might instead be of halos with unusual radii produced (geometrically) by pyramidal crystals; a particularly striking example was analyzed by Neiman.[8]

Given the different mechanisms for the minimum deviation, it is not surprising that the forms of the diffraction cross sections turn out to be different for halos than for rainbows, but it is a little surprising that the halo cross sections share the rainbow property of depending on functions of a single variable, which can be evaluated in closed form. The universal halo functions are calculated for two idealized crystal orientation distributions, called case I and case II. In case I (Section 3) plate crystals share a common axis perpendicular to the incident beam, and their orientation depends on a single angle describing rotation about this axis; this distribution corresponds

The author is with the H. H. Wills Physics Laboratory, University of Bristol, Royal Fort, Tyndall Avenue, Bristol, Avon BS8 1TL, UK.

Received 12 July 1993; revised manuscript received 18 October 1993.

0003-6935/94/214563-06$06.00/0.

to parhelia (sun dogs). In case II (Section 4), the axes too are randomly oriented; for pencil crystals this distribution corresponds to the common 22° halo. Both halo diffraction functions are compared with their rainbow counterpart, and their properties are used to show why supernumerary halos are not common.

2. Geometric Singularities

Attention is restricted to an idealized model involving refraction by (truncated) 60° prisms in randomly oriented hexagonal crystal columns or plates. A collimated beam of monochromatic light strikes a prism face oriented near minimum deviation. Only directions close to minimum deviation are considered, so the variation of the Fresnel reflection coefficient can be ignored. Polarization effects[9,10] are also ignored.

In case I, all crystals share a common (vertical) symmetry axis that is parallel to the edges of the effective 60° prisms. The prisms are randomly rotated about their edges. Assume for simplicity that the incident sunlight is perpendicular to the edges, i.e., horizontal or almost so, so there are no skew rays. (The theory is almost the same for higher Sun elevations when there are skew rays; the essential point is the common axis, which ensures that the skewness is constant.) Let the angle of incidence on a crystal be

$$i = i_{\min} + \psi, \tag{1}$$

where $i_{\min}$ ($\approx 40.92°$ for the refractive index 1.31 corresponding to yellow light) corresponds to minimum deviation, and ψ, which describes the orientation, is small. The deviation angle of the emergent beam is

$$D_{\text{geom}} = D_{\min} + A\psi^2 + \text{higher terms}, \tag{2}$$

where $D_{\min}$ is the geometric halo angle (i.e., the minimum deviation, equal to 21.84°) and A is a constant.

Each crystal contributes a beam described by a delta function in the direction D_{geom}, so the intensity generated by the whole collection is the average over orientations ψ. This is

$$\langle I_{\text{geom, I}}(D)\rangle = \int_{-\infty}^{\infty} d\psi\, \delta(D - D_{\min} - A\psi^2) = \frac{1}{[A(D - D_{\min})]^{1/2}}\, \Theta(D - D_{\min}), \tag{3}$$

where Θ denotes the unit step (the integration range has been extended to infinity because the only significant orientations are those near minimum deviation, where it is essential that the orientation distribution is smooth). The singularity here, at each of the minimum deviation spots on either side of the Sun (i.e., the parhelia), is exactly the same as that at the caustic line of the rainbow, in spite of the two different mechanisms for the formation of this singularity.

In case II, the axes of the prisms are random as well, so that it is necessary to consider skew rays. An important observation, first made clearly by Können,[9] is that this alters the nature of the singularity. Let the prism axis make an angle $\chi + \pi/2$ with the incident direction; thus χ measures the skewness. The deviation angle now depends on χ as well as on ψ, but not on the third angle that specifies the orientation of the prism, say, ϕ, which describes rotations of the edge about the incident direction. It is known[1] that

$$D_{\text{geom}} = D_{\min} + A\psi^2 + B\chi^2 + \text{higher terms}. \tag{4}$$

Instead of Eq. (3), we have

$$\langle I_{\text{geom, II}}(D)\rangle = \int_{-\infty}^{\infty} d\psi \int_{-\infty}^{\infty} d\chi\, \delta(D - D_{\min} - A\psi^2 - B\chi^2) = \frac{\pi}{(AB)^{1/2}}\, \Theta(D - D_{\min}). \tag{5}$$

Because of the randomness in ϕ, this singularity forms a circular arc around the Sun, which is, of course, the 22° halo. The fact that the singularity is weaker—a finite step rather than a divergence—is a reason why these halos are less prominent than rainbows (another reason is that halos, unlike rainbows, are on the bright side of the sky).

3. Diffraction for Case I (Parhelia)

Now we assume that the wavelength λ of the light is much smaller than the crystal diameter d (assumed the same for all crystals). In the simplest approximation, diffraction spreads the beams emerging from each crystal, the spreading in D being that from a slit whose width is approximately $w = d \cos i_{\min}/2 \approx 0.38d$. Thus the intensity from a given crystal is proportional to

$$I(D) = \frac{w}{\lambda}\left\{\frac{\sin[\pi w(D - D_{\text{geom}})/\lambda]}{\pi w(D - D_{\text{geom}})/\lambda}\right\}^2. \tag{6}$$

[The normalization is chosen to make $I(D) \to \delta(D - D_{\text{geom}})$ in the geometric-optics limit $\lambda \to 0$.]

For case I we have, instead of the geometric average of Eq. (3), the diffraction intensity

$$\langle I_{\text{I}}(D)\rangle = \frac{w}{\lambda}\int_{-\infty}^{\infty} d\psi \left\{\frac{\sin[\pi w(D - D_{\min} - A\psi^2)/\lambda]}{\pi w(D - D_{\min} - A\psi^2)/\lambda}\right\}^2. \tag{7}$$

Scaling now gives

$$\langle I_{\text{I}}(D)\rangle = \left(\frac{\pi w}{\lambda A}\right)^{1/2} p(\eta), \tag{8}$$

where

$$\eta \equiv \frac{1.187(D - D_{\min})d}{\lambda},$$

$$p(\eta) \equiv \frac{1}{\pi}\int_{-\infty}^{\infty} du\left[\frac{\sin(\eta - u^2)}{\eta - u^2}\right]^2. \qquad (9)$$

Note that $\eta > 0$ corresponds to the geometrically bright sides of the parhelia. This gives the horizontal spreading across the geometric edge. [There will also be diffraction in the vertical, described by the same function as Eq. (6), with w replaced by the thickness of the crystal plates; this is not considered further.]

The function $p(\eta)$ is the parhelion analog of the Airy function, and we now examine its properties. First note that it depends on a single scaling variable η that does not involve the parameter A describing the sharpness of the minimum deviation. Second, note that a change of the integration variable gives

$$p(\eta) \equiv \frac{1}{\pi}\int_{-\eta}^{\infty} \frac{d\nu}{(\nu + \eta)^{1/2}}\left(\frac{\sin \nu}{\nu}\right)^2, \qquad (10)$$

showing that the cross section is the geometric singularity convolved with the slit diffraction function. Third, this observation enables $p(\eta)$ to be evaluated in closed form because the Fourier transforms of both components are known. A calculation gives

$$p(\eta) = \frac{\cos\left(2\eta + \frac{\pi}{4}\right)}{\eta(2\pi)^{1/2}} + \frac{1}{2\sqrt{\pi}}\left\{\left(2 - \frac{1}{2\eta}\right)C\left[2\left(\frac{|\eta|}{\pi}\right)^{1/2}\right] + \operatorname{sign}(\eta)\left(2 + \frac{1}{2\eta}\right)S\left[2\left(\frac{|\eta|}{\pi}\right)^{1/2}\right]\right\}, \qquad (11)$$

where C and S denote the Fresnel integrals[2] defined by

$$C(z) + iS(z) \equiv \int_0^z dt \exp\left(i\frac{\pi}{2}t^2\right). \qquad (12)$$

Fourth, the following limiting forms can easily be found from Eq. (11):

$$p(\eta) \approx \frac{1}{\sqrt{\eta}} - \frac{\sin\left(2\eta + \frac{\pi}{4}\right)}{4\eta^2(2\pi)^{1/2}} \qquad (\eta \gg 1),$$

$$= \frac{4}{3\sqrt{\pi}} \qquad (\eta = 0),$$

$$\approx \frac{1}{4|\eta|^{3/2}} - \frac{\sin\left(2\eta + \frac{\pi}{4}\right)}{4\eta^2(2\pi)^{1/2}} \qquad (\eta \ll -1) \qquad (13)$$

The terms that give rise to the geometric-optics singularity of Eq. (3) in the limit $\lambda \to 0$ [after the scalings of Eqs. (8) and (9)] are

$$p(\eta) \sim \frac{1}{\sqrt{\eta}} \qquad (\eta > 0),$$

$$\sim 0 \qquad (\eta < 0). \qquad (14)$$

The sine terms in expressions (13) describe supernumerary parhelia; note that these occur on both sides of the geometric edge $\eta = 0$.

Fifth, the graph of $p(\eta)$ (Fig. 1) indicates that the supernumerary parhelia are of very low contrast and barely visible on the bright side ($\eta > 0$) of the halo. Even on the dark side, the maximum contrast is only $(p_{\max} - p_{\min})/(p_{\max} + p_{\min}) = 0.178$ (these values refer to the first minimum at $\eta = -2.949$ and the first subsidiary maximum at $\eta = -4.020$).

There are several striking differences between the parhelion function $p(\eta)$ and its rainbow analog (insets in Fig. 1), namely, $\mathrm{Ai}^2(-\rho)$, where,[11] for a drop of refractive index n and diameter d,

$$\rho = (D - D_{\min})\frac{(n^2 - 1)^{1/2}}{(4 - n^2)^{1/6}}\left(\frac{2\pi d}{3\lambda}\right)^{2/3}. \qquad (15)$$

First, supernumerary rainbows occur only on the

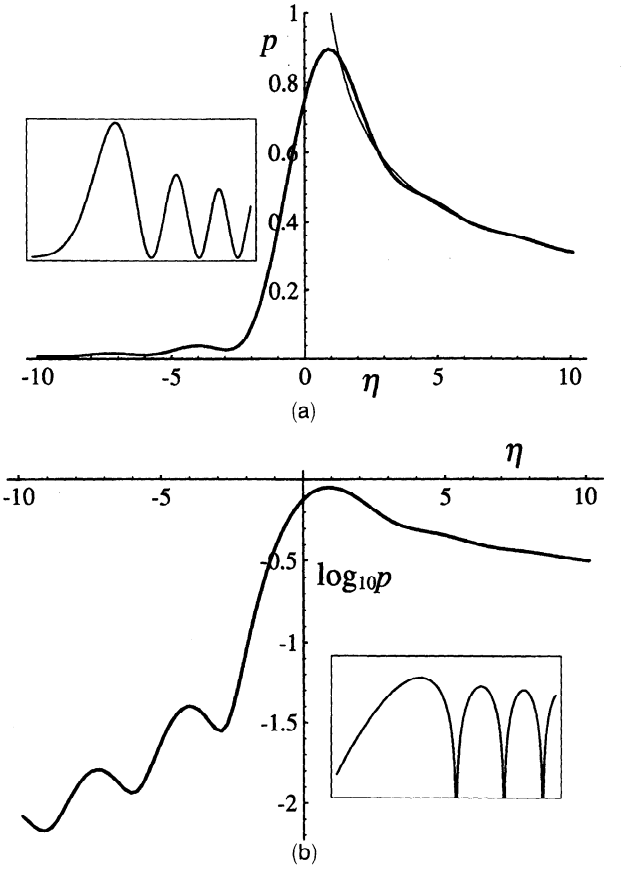

Fig. 1. (a) Thick curve, universal parhelion diffraction function $p(\eta)$ [Eq. (11)]; thin line; geometric-optics approximation [approximation (14)]; inset, the corresponding rainbow function $\mathrm{Ai}^2(-\rho)$. (b) Logarithm of $p(\eta)$: inset, logarithm of $\mathrm{Ai}^2(-\rho)$.

bright side of the geometric caustic, whereas there are supernumerary parhelia on both sides of the edge, with higher contrast on the dark side (Fig. 1).

Second, the separation of supernumerary rainbows scales as $\lambda^{2/3}$, whereas that of supernumerary parhelia scales as λ, so parhelion fringes are much closer than rainbow fringes for a crystal and a drop with the same diameter d (provided $d \gg \lambda$). The separation of the first two Airy intensity maxima is

$$\Delta D = 1.7641 \left(\frac{\lambda}{d}\right)^{2/3}, \tag{16}$$

whereas parhelion fringe maxima are separated by [cf. Eq. (9) with $\Delta\eta = \pi$]

$$\Delta D = 2.647 \frac{\lambda}{d} \tag{17}$$

An important value is $\Delta D = 0.5°$, the diameter of the Sun, which happens to be similar to $\Delta D \sim 0.6°$ for the geometric color broadening arising from refractive dispersion. Then, for $\lambda = 600$ nm, Eq. (16) shows that supernumerary rainbows are quenched for drops larger than $d \sim 1.7$ mm, whereas Eq. (17) shows that supernumerary parhelia are eliminated for crystals larger than $d \sim 0.18$ mm. However, it is known[12] that halos (and, presumably, parhelia as well) can be formed by crystals several times smaller than this, so their supernumeraries would not be quenched in this way.

Third, the contrast of rainbow fringes is much greater than that of parhelia. The minima of $\mathrm{Ai}^2(-\rho)$ are zeros, so supernumerary rainbows have contrast unity. On the other hand, we have seen that the contrast of parhelion fringes is at most 0.178. The low value means that supernumerary parhelia are more vulnerable to quenching by variations in the size of ice crystals. I think this is the main reason why supernumeraries are not normally seen in parhelia, whereas supernumerary rainbows are frequently seen (especially near the rainbow top[13]). However, supernumerary parhelia ought to be observable in the laboratory, for example in monochromatic collimated light scattered by a small rapidly spinning prism or crystal.

Fraser[14] shows simulations of the intensity distribution across the 22° halo for different sizes of crystal, using the same physical theory as that presented here for parhelia (and in particular neglecting skew rays), with the additional feature that the variation of the Fresnel coefficients is included. Measurements on his Fig. 2 show that his logarithmic curves can be scaled with the variables of Eqs. (9) to fit the universal formula of Eq. (11) and so have the universal shape of Fig. 1(b).

4. Diffraction for Case II (22° Halos)

To include skew rays, we simply replace the delta function in the geometric average of Eq. (5) by the slit diffraction function of Eq. (6). This gives

$$\langle I_{\mathrm{II}}(D)\rangle = \frac{w}{\lambda}\int_{-\infty}^{\infty} d\psi \int_{-\infty}^{\infty} d\chi \left\{\frac{\sin[\pi w(D - D_{\mathrm{geom}})/\lambda]}{\pi w(D - D_{\mathrm{geom}})/\lambda}\right\}^2. \tag{18}$$

After scaling [cf. Eq. (8)], we obtain

$$\langle I_{\mathrm{II}}(D)\rangle = \frac{\pi}{(AB)^{1/2}} h(\eta), \tag{19}$$

where η is as given in Eqs. (9), and $h(\eta)$ is

$$h(\eta) = \frac{1}{\pi^2}\int_{-\infty}^{\infty} du \int_{-\infty}^{\infty} dv \left[\frac{\sin(\eta - u^2 - v^2)}{\eta - u^2 - v^2}\right]^2. \tag{20}$$

This is the universal halo function that describes diffraction softening of the geometric step of Eq. (5), whose properties are now examined. First note that $h(\eta)$ depends on a single scaling variable η, which does not involve the parameters A and B describing the sharpness of the minimum deviation. Second, the function is easily evaluated by transforming to polar coordinates in the u, v plane and integrating by parts. The result is

$$h(\eta) = \frac{1}{2} - \frac{\sin^2\eta}{\pi\eta} + \frac{\mathrm{Si}(2\eta)}{\pi}, \tag{21}$$

where Si denotes the sine integral[2] defined by

$$\mathrm{Si}(z) \equiv \int_0^z dz \frac{\sin z}{z}. \tag{22}$$

Third, the limiting forms are

$$\begin{aligned} h(\eta) &\approx 1 - \frac{1}{2\pi\eta} - \frac{\sin(2\eta)}{2\pi\eta^2} && (\eta \gg 1), \\ &= 1/2 && (\eta = 0), \\ &\approx -\frac{1}{2\pi\eta} - \frac{\sin(2\eta)}{2\pi\eta^2} && (\eta \ll -1). \end{aligned} \tag{23}$$

These limits incorporate the geometric step, as, from Eqs. (9), small λ implies large $|\eta|$. The sine terms in Eqs. (23) describe the supernumerary halos. As with parhelia, these occur on both sides of the step, at $\eta = n\pi$ $(n \neq 0)$.

Fourth, the supernumeraries are shoulders, that is zero-slope inflections, rather than maxima. This is because Eq. (21) implies

$$\frac{d}{d\eta} h(\eta) = \frac{\sin^2\eta}{\pi\eta^2}, \tag{24}$$

which is never negative. These faint supernumerary fringes can be seen in the graphs of $h(\eta)$ and $\log h(\eta)$ (Fig. 2).

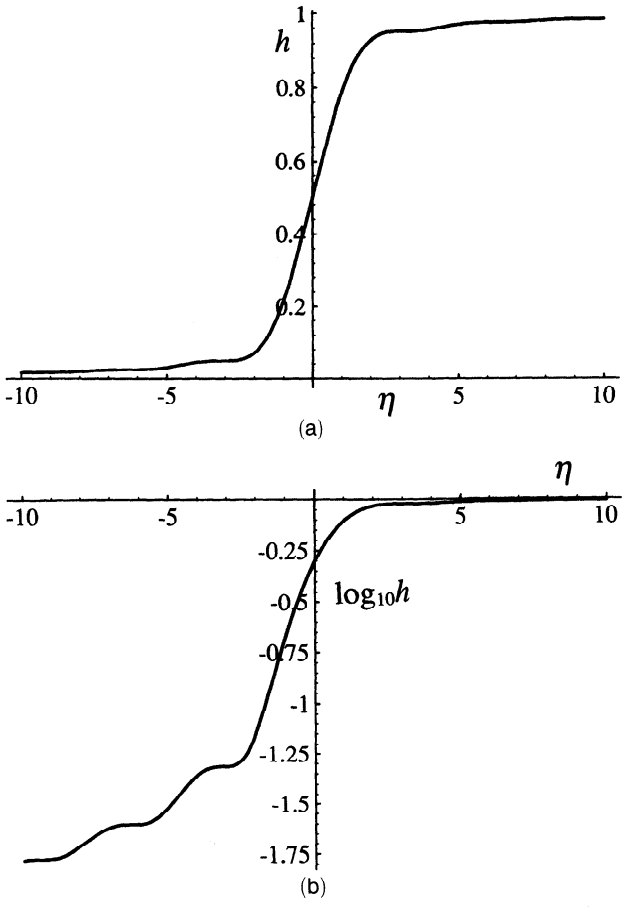

Fig. 2. (a) Universal halo diffraction function $h(\eta)$ [Eq. (21)], (b) logarithm of $h(\eta)$.

The remarks in the penultimate three paragraphs of Section 3, which contrast supernumerary parhelia with their rainbow counterparts, also apply to the supernumerary halos described by $h(\eta)$. Indeed, the argument that supernumerary parhelia are unlikely to be observed because of their low contrast applies more strongly to supernumerary halos, because, as has just been explained, these have zero intensity contrast.

5. Concluding Remarks

Using idealized models for the simplest cases, I have calculated halo difraction functions in the asymptotic regime of directions close to the geometric singularities for crystals that are large in comparison with the wavelength of light, and I have argued that the supernumerary fringes predicted by these functions are too weak to be observed. The fringes will be even weaker in circumstances in which these idealizations break down, such as crystals larger than 0.18 mm, large variations in crystal size, or[7] variations in the angles between crystal faces that occur while crystals are growing.

But supernumeraries are not the only effect of diffraction. Another is broadening of the main maximum onto the geometrically dark side. From Figs. 1 and 2 this is of the same order of magnitude as that of Eq. (17) and so is probably visible, as Visser argued,[5,6] in spite of broadening from the Sun and dispersion, for crystals smaller than $d \sim 0.18$ mm, even when the supernumerary parhelia and halos are obscured by variations in crystal size.

More generally, it is interesting to consider the geometry of halos and related phenomena from the standpoint of singularity theory. I think that this subject is not completely understood, although considerable progress has been made by Tape.[15,16] In the case of caustics, that is, focal singularities of smooth families of rays, of which the rainbow is an example, the singularities are those of catastrophe theory.[17] This provides a classification that enables complicated caustics to be understood. We can ask whether the same mathematics can be employed to classify more complicated halos. It cannot. Although both caustics and halos are singularities of smooth maps, the map for halos (linking crystal orientation to beam deflection) is not of the gradient type assumed in catastrophe theory. In two dimensions (that is, on the sky) all smooth maps share line and cusp singularities, and some halos do indeed show cusps.[15,16] But with additional parameters (such as the elevation of the Sun), the singularities of gradient and nongradient mappings are different.[18] Therefore we do not expect to see halos involving some of the higher catastrophes, such as umbilics, or sections close to their singularities. However, swallowtail singularities are stable in both gradient and nongradient maps from $R^3 \rightarrow R^3$, and it is surprising that neither this singularity nor its characteristic two-cusped, self-crossing section appears in any of the numerous simulations of halos.

A related problem concerns the circumstances in which the geometric intensity singularities are steps or inverse-square-root divergences or singularities of another sort. I agree with Können and Tinbergen's conjecture[10] that the step is the generic case. For example, the inverse square root for parhelia is unstable in the sense that it is replaced by a (large) step if there is any randomness in the distribution of crystal axis directions (physically, this instability is important only if the variation in direction exceeds the diffraction spreading of the singularity).

Finally, it is worth noting that caustics and the halo mechanisms elaborated here do not exhaust the possibilities for producing geometric singularities. For example, it appears that the inverse-square-root singularity shared by rainbows and parhelia can also arise directly from a singularity in the distribution of crystal orientations, as in the rare Bottlinger's rings, formed by reflection, around the subsun.[19]

I thank R. G. Greenler for encouraging me to carry out the calculation reported here, G. P. Können for pointing out a serious error in an early version of this paper and for some helpful references, and J. F. Nye for a thorough reading of the manuscript and several suggestions.

References

1. R. A. R. Tricker, *Introduction to Meteorological Optics* (Elsevier, New York, 1970), Chap. 4.
2. R. Greenler, *Rainbows, Halos and Glories* (Cambridge U. Press, Cambridge, 1980).
3. M. Abramowitz and I. A. Stegun, *Handbook of Mathematical Functions* (National Bureau of Standards, Washington, D.C., 1964), Sec. 10.4.
4. M. G. J. Minnaert, *Light and Color in the Outdoors* (Springer, New York, 1993), p. 212.
5. S. W. Visser, "Over de Buiging van het Licht bij de Vorming van Halo's," K. Ned. Akad. Wet. Versl. Gewone Vergad. Afd. Natuurkd. **25,** 1328–1351 (1918).
6. S. W. Visser, "Die Halo-Erscheinungen," in *Handbuch der Geophysik,* F. Linke and F. Möller, eds. (Springer-Verlag, Berlin, 1961), Vol. 8, Chap. 15, pp. 1027–1081.
7. G. P. Können, Royal Netherlands Meteorological Society, De Bilt, The Netherlands (personal communication, 1993).
8. P. J. Neiman, "The Boulder, Colorado, concentric halo display of 21 July 1986," Bull. Am. Meteorol. Soc. **70,** 258–264 (1989).
9. G. P. Können, "Polarisation and intensity distributions of refraction halos," J. Opt. Soc. Am. **73,** 1629–1640 (1983).
10. G. P. Können and J. Tinbergen, "Polarimetry of a 22° halo," Appl. Opt. **30,** 3382–3400 (1991).
11. H. M. Nusssenzveig, *Diffraction Effects in Semiclassical Scattering* (Cambridge U. Press, Cambridge, 1992), p. 108.
12. W. Tape, "Some ice crystals that made halos," J. Opt. Soc. Am. **73,** 1641–1645 (1983).
13. A. B. Fraser, "Why can the supernumerary bows be seen in a rain shower?" J. Opt. Soc. Am. **73,** 1626–1628 (1983).
14. A. B. Fraser, "What size of ice crystals causes the halos?" J. Opt. Soc. Am. **69,** 1112–1118 (1979).
15. W. Tape, "Geometry of halo formation," J. Opt. Soc. Am. **69,** 1122–1132 (1979).
16. W. Tape, "Analytic foundations of halo theory," J. Opt. Soc. Am. **70,** 1175–1192 (1980).
17. M. V. Berry and C. Upstill, "Catastrophe optics: morphologies of caustics and their diffraction patterns," Prog. Opt. **18,** 258–346 (1980).
18. A. Thorndike, C. R. Cooley, and J. F. Nye, "The structure and evolution of flow fields and other vector fields," J. Phys. A **11,** 1455–1490 (1978).
19. D. K. Lynch and F. C. Mertz, "Bottlinger's rings," in *Light and Color in the Open Air,* Vol. 13 of 1993 OSA Technical Digest Series (Optical Society of America, Washington, D.C., 1993), pp. 73–75.